LH Transition by a Biased Hot Cathode in the Tohoku University Heliac

S. Kitajima[1)], H. Takahashi[1)], Y. Tanaka[1)], H. Utoh[1)], M. Sasao[1)], M. Takayama[2)],
K. Nishimura[3)], S. Inagaki[3)] and M. Yokoyama[3)]

1) *Department of Quantum Science and Energy Engineering, Tohoku University, Sendai, 980-8579, Japan*
2) *Akita Prefectural University, Honjyo, Akita, 015-0055, Japan*
3) *National Institute for Fusion Science, Toki, Gifu 509-5292, Japan*

Outline

- Introduction
- Experimental set-up for a hot cathode biasing in Tohoku University Heliac
- Electrode biasing experiments of *constant voltage*
- Electrode biasing experiments of *current sweep*
- Summary

Introduction

Background

- In theories for L-H transition, the local maximum in ion viscosity against poloidal Mach number around $-M_p$ = 1 - 3 is considered to play the key role.
  This maximum is considered to be related to the toroidicity.
- Universal features among tokamaks and stellarators in L-H transition can be studied if this poloidal mach number M_p region is investigated in detail.

Purposes

- Research on the characteristics of biased plasmas in TU-Heliac.
- Feasibility study of active control of the $\boldsymbol{J} \times \boldsymbol{B}$ driving force for the poloidal rotation by the current sweep biasing
- Estimation of the ion viscous damping forces from the $\boldsymbol{J} \times \boldsymbol{B}$ driving forces
- Comparison between the measured ion viscous damping force and the neoclassical predictions

Tohoku University Heliac (TU-Heliac)

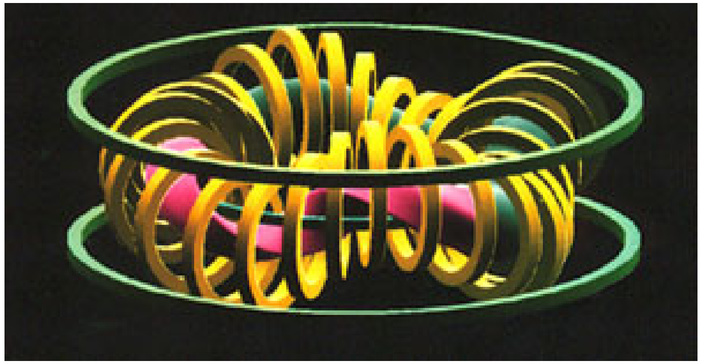

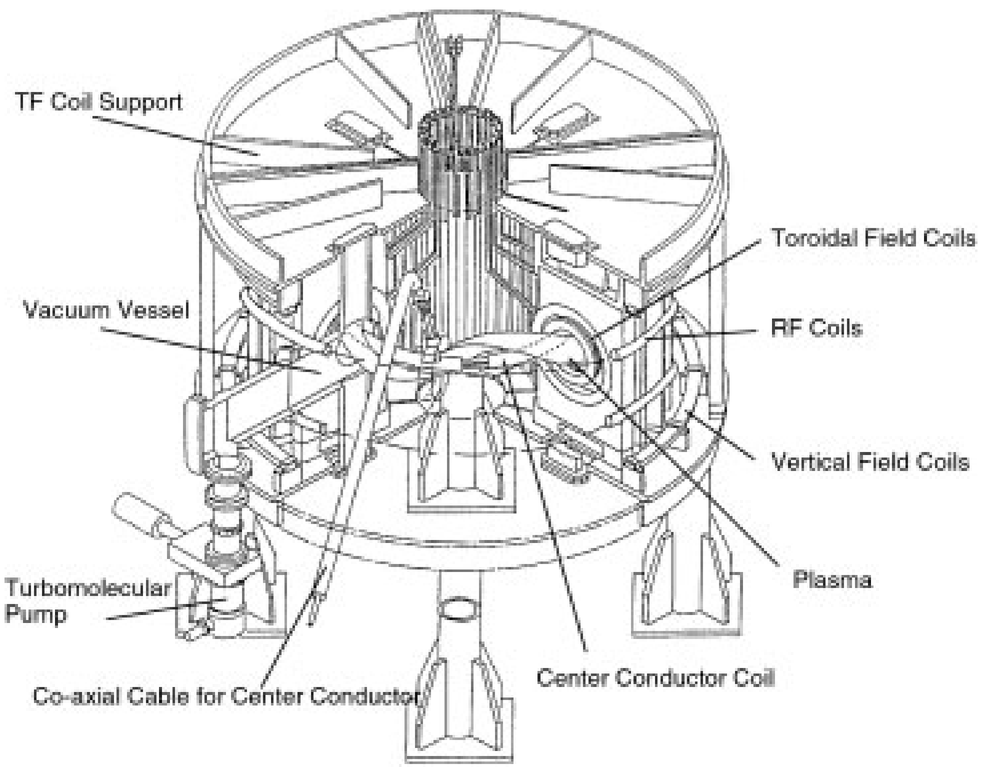

Bird's-eye view of the Tohoku University Heliac

Machine and Plasma Parameters

Number of field periods	4
Major radius	48 cm
Average radius of the last closed flux surface r_{LCFS}	7 cm
Magnetic field on axis B_0	0.3 T
Rotational transform	1.54 - 1.71
Well depth	3 %
RF frequency f_{RF}	18.8 kHz
RF output power P_{RF}	35 kW
Residual gas pressure	~ 5 x 10^{-6} Pa

Experimental set-up

Working gas	He (1.2×10^{-2} Pa)
Electron density on axis N_{e0}	6×10^{11} cm^{-3}
Electron Temperature on axis T_{e0}	~ 25eV
RF frequency f_{RF}	18.8 kHz

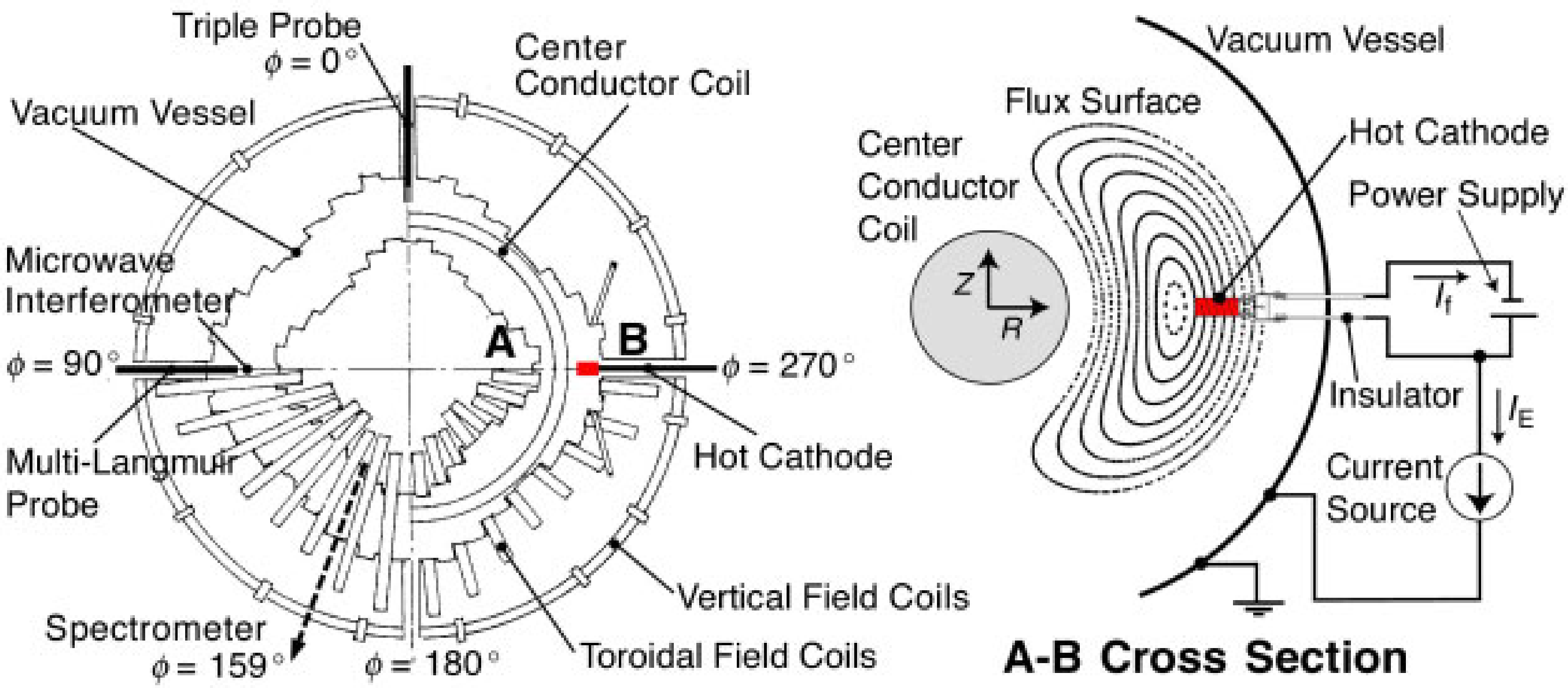

The hot cathode is inserted horizontally from the low field side.
Negative bias voltage is applied against to the vacuum vessel.

Characteristics of biased plasma with *Constant Voltage* (1)

Typical time evolution of the plasma parameters with a *constant voltage* biasing

- Strong negative E_r and E_r shear were formed.
- Line density increased by a factor of 2 ~ 3.
- Fluctuation level of floating potential $e\tilde{V}_f / \bar{T}_e$
  Fluctuation level of saturation current $\tilde{I}_s / \bar{I}_s$
  → Suppressed.
- Normalized impurity light emission (H_α) decreased.

The biased plasma shows the same characteristics as the H-mode in large tokamaks and stellarators.

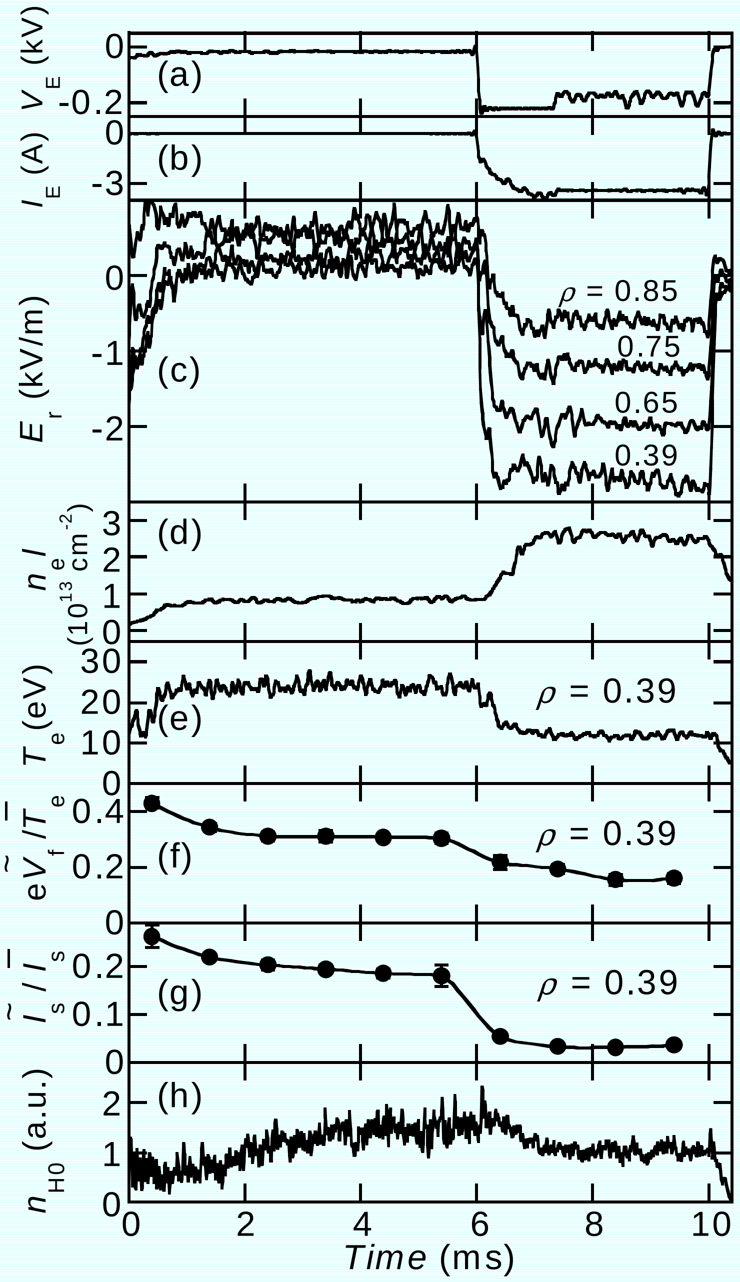

Characteristics of biased plasma with *Constant Voltage* (2)

Dependence of the stored energy on the input power through the hot cathode

The stored energy was plotted against the hot cathode input power.

- ✧ The electrode voltage actively changed.
- ✧ The stored energy: the product of the density and the electron temperature.
- ✧ The input power: the product of the electrode voltage and electrode current.
- ✧ The input power of the low frequency joule heating was kept constant.

- The linear gradient after the transition was about twice larger than that before the transition.

  This suggests the energy confinement time increases by a factor of 2.

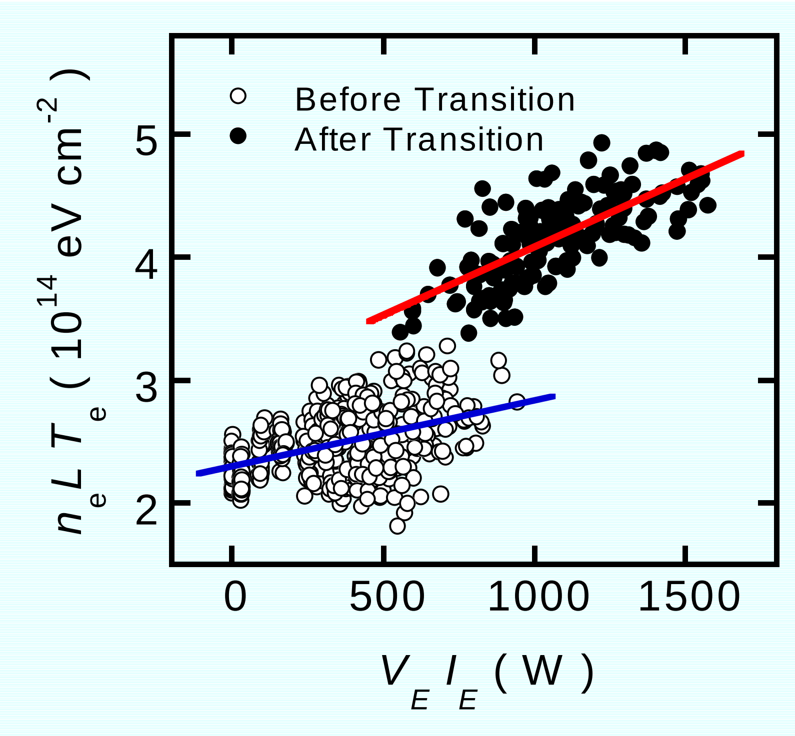

$P_{\mathrm{Input}} = P_{\mathrm{Joule\ heating}} + P_{\mathrm{Hot\ Cathode}}$

$P_{\mathrm{Joule\ heating}} = \mathrm{constant}$

This observation also indicates the same characteristics as the H-mode in large tokamaks and stellarators.

Characteristics of biased plasma with *Current Sweep*

Typical time evolution of the plasma parameters with current sweep

The electrode current I_E was kept constant at ~ 4 ampere from 0 to 5 msec and then ramped down from 5 to 10 msec

- The electric fields in outer region decreased gradually according to the electrode current I_E.
- The improved mode continued until ~7 msec
  - ✧ The line density was sustained high level.
  - ✧ The floating potential fluctuation level
    The saturation current fluctuation level
    → suppressed.
- Plasma shows *negative resistance* between A and B.
- The electrode current I_E bifurcates to an electrode voltage V_E.

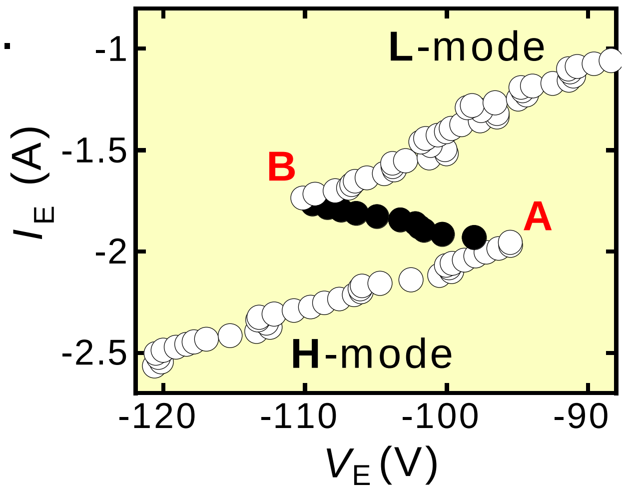

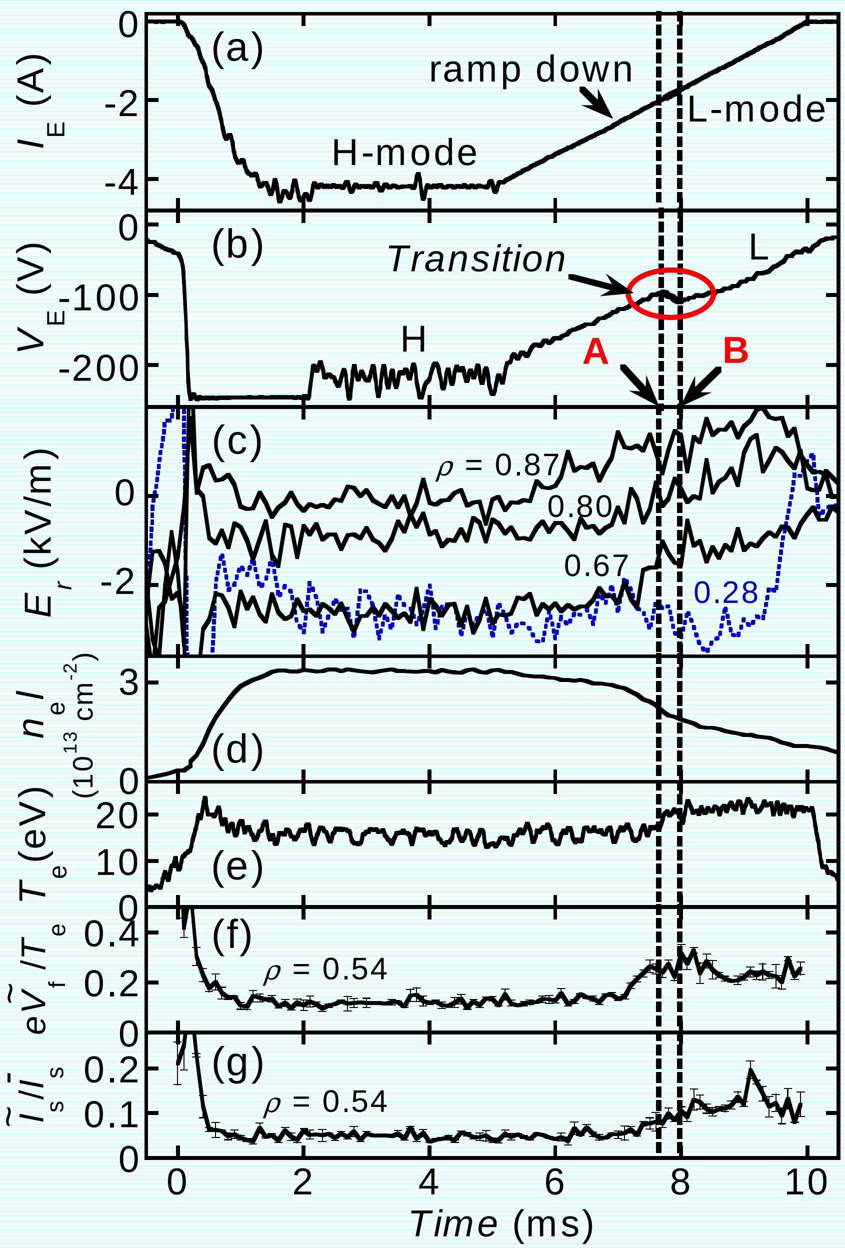

Feasibility study of active control of driving force with *current sweep* (1)

Dependence of radial electric field E_r on the electrode current I_E

- Radial electric field E_r (except around the magnetic axis) was almost linearly proportion to the electrode current I_E in both the current ramp up and ramp down cases.

This indicates the capability of active control of the driving force for the poloidal rotation.

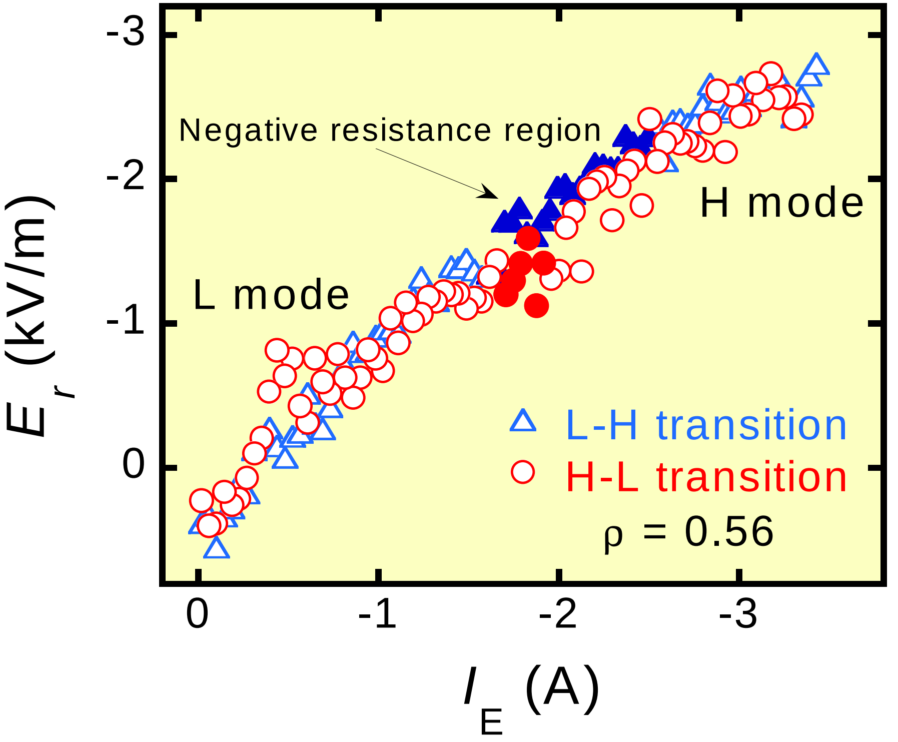

Feasibility study of active control of driving force with *current sweep* (2)

Measurements of the fluctuation level of ion saturation currents by a multi-Langmuir probe

→ Demonstration of active control of the $\boldsymbol{J} \times \boldsymbol{B}$ driving force for the poloidal rotation by externally controlled electron injection

- The frequency range spread from 80 kHz to 130 kHz.
- All signals were kept a similar time evolution and had a phase shift according to the poloidal locations.
- The estimation of the poloidal rotation velocities from the phase shift
  The rotation velocities were widely changed by the actively controlled electrode current sweep and agreed with the $\boldsymbol{E} \times \boldsymbol{B}$ drift velocities.

This also indicates the capability of active control of the driving force for the poloidal rotation.

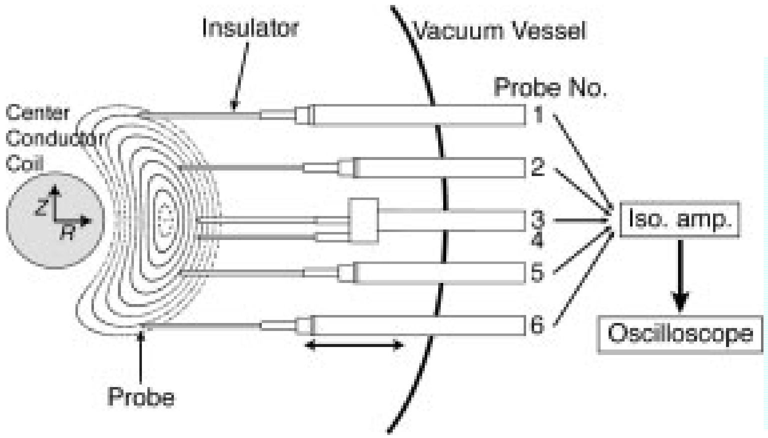

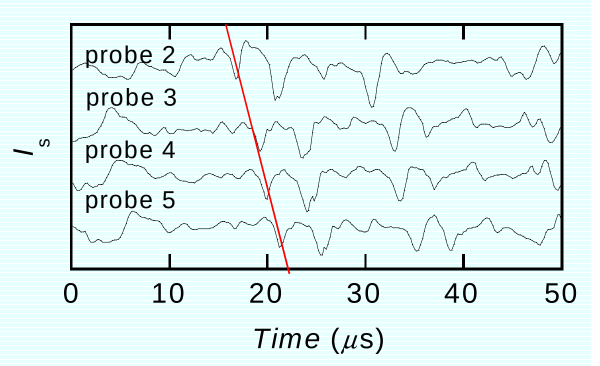

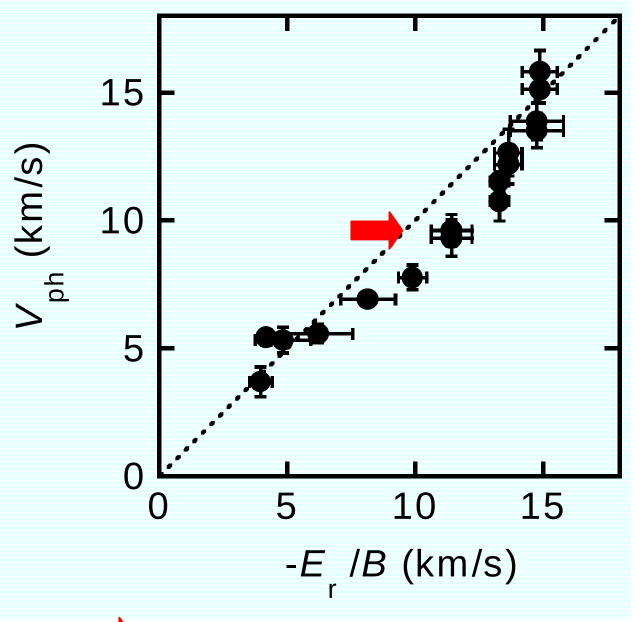

This discrepancy can be eliminated by the ion diamagnetic drift velocity.

Estimation of ion viscous damping force (1)

- **Momentum Balance Equation in steady state**

$$\underbrace{< J_\rho > B_0}_{(1)\ \boldsymbol{J} \times \boldsymbol{B}} = -\underbrace{\frac{<\vec{B}\cdot\nabla\cdot\vec{\vec{\pi}}_{\mathrm{i}}>}{\Theta B_0}}_{(2)\ \text{viscosity}} \underbrace{- (1+2q^2) n_{\mathrm{i}} m_{\mathrm{i}} \nu_{\mathrm{in}} V_\theta}_{(3)\ \text{friction}}$$

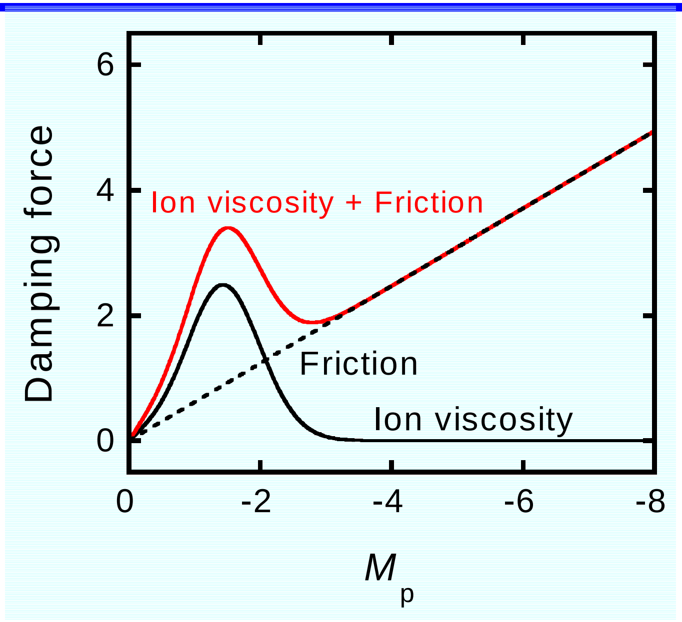

(1) $$< J_\rho > B_0 \Rightarrow \frac{B_0}{\sqrt{\pi}\,2\pi L} I_{\mathrm{E}} p_{\mathrm{i}}^{-1} \varepsilon^{-2}, \quad < J_\rho > = \frac{I_{\mathrm{E}}}{2\pi < r > L}$$

(2) $$\frac{<\vec{B}\cdot\nabla\cdot\vec{\vec{\pi}}_{\mathrm{i}}>}{\Theta B_0} \Rightarrow \underbrace{M_{\mathrm{p}}(M_{\mathrm{p}} + 2M_{\mathrm{p}}^2 + 2M_{\mathrm{p}}^4)\exp(-M_{\mathrm{p}}^2)}_{\text{Rozhansky model}^{(1)}};$$

local maximum exists for M_{p}

(3) $$(1+2q^2) n_{\mathrm{i}} m_{\mathrm{i}} \nu_{\mathrm{in}} V_\theta \Rightarrow \frac{2}{\sqrt{\pi}} \frac{1+2q^2}{q^2} \frac{\nu_{\mathrm{in}} R_0 q}{v_{\mathrm{th}}} M_{\mathrm{p}};$$

proportional to M_{p}

$< J_\rho >$; surface averaged radial current density, B_0 ; magnetic field on axis, $\vec{\vec{\pi}}_{\mathrm{i}}$; ion viscosity stress tensor, $\Theta = B_\theta / B_\phi$, q ; safety factor, $\nu_{\mathrm{in}} = < \sigma_{\mathrm{cx}} u_{\mathrm{i}} > n_{\mathrm{n}}$, V_θ ; surface averaged poloidal flow velocity, L ; length of the magnetic axis, ε ; toroidal ripple, $M_{\mathrm{p}} = V_\theta / \Theta v_{\mathrm{th}}$, $v_{\mathrm{th}} = (2T_{\mathrm{i}} / m_{\mathrm{i}})^{1/2}$, R_0 ; major radius

(1) V. Rozhansky and M. Tendler: Phys. Fluids B 2 (1992) 1877.

Estimation of ion viscous damping force (2)

The ion viscous damping force opposing to the poloidal rotation was estimated from the externally controlled driving force for the ***J*** x ***B*** poloidal rotation, and compared with the neoclassical predictions.

- The measured damping force had a local maximum at the poloidal Mach number M_p ~ - 1.5 and agreed well with the neoclassical predictions.
  (We assumed that the ion temperature $T_i = 0.2T_e$.)
- The plasma showed the negative resistance characteristics (closed symbol ■) in the region where the ion viscous damping force had a local maximum.

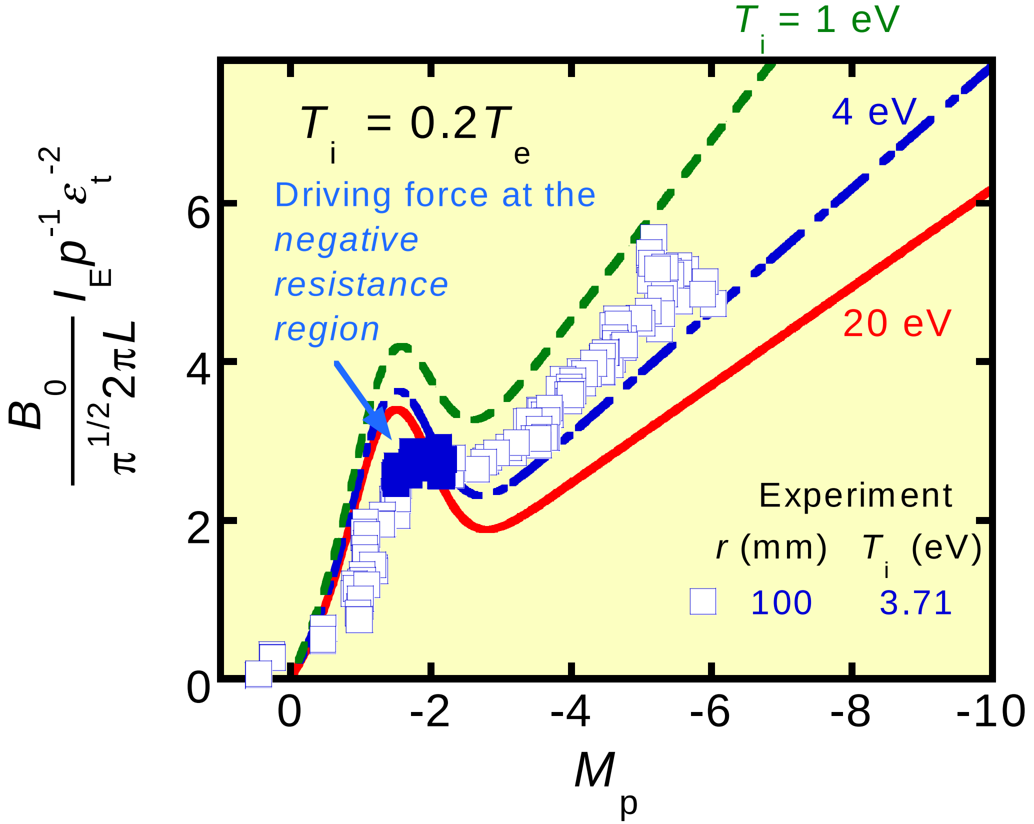

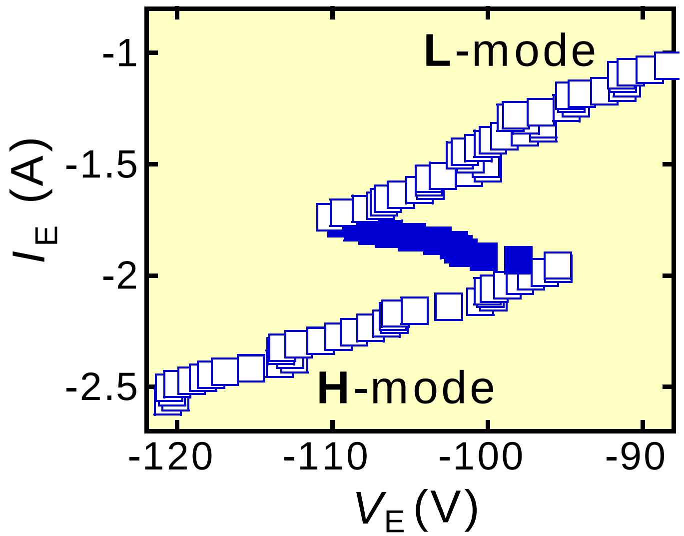

Estimation of ion viscous damping force (3)

Effect of collisionality to the damping force

In the high M_p region ($-M_p > 3$), the dominant damping force to the poloidal rotation is the friction to neutral particles.

- The negative resistance region can be seen at all filling gas pressure cases.
- The measured viscous damping forces had a local maximum at $-M_p \sim 1.5$ at all cases and agreed well with the neoclassical predictions at low pressures, *i.e.*, in case of lower collisionality.
- Regions of the negative resistance ($1 < -M_p < 2$) are independent on collisionality, although the electrode parameters were quite different.

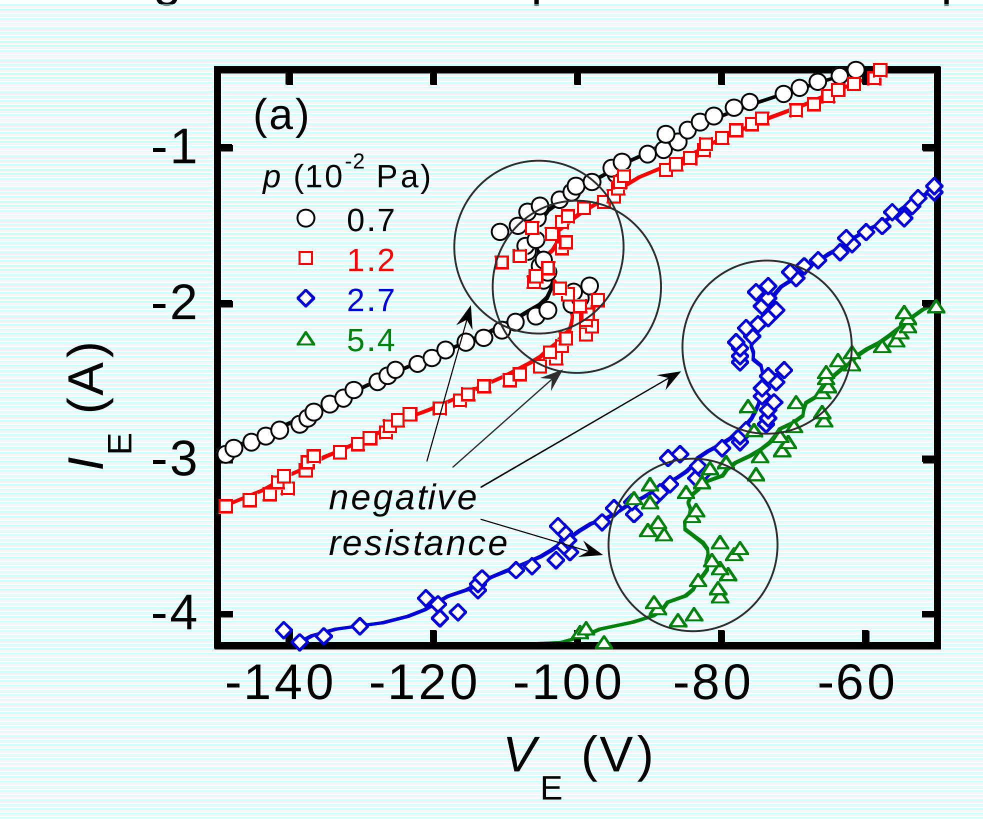

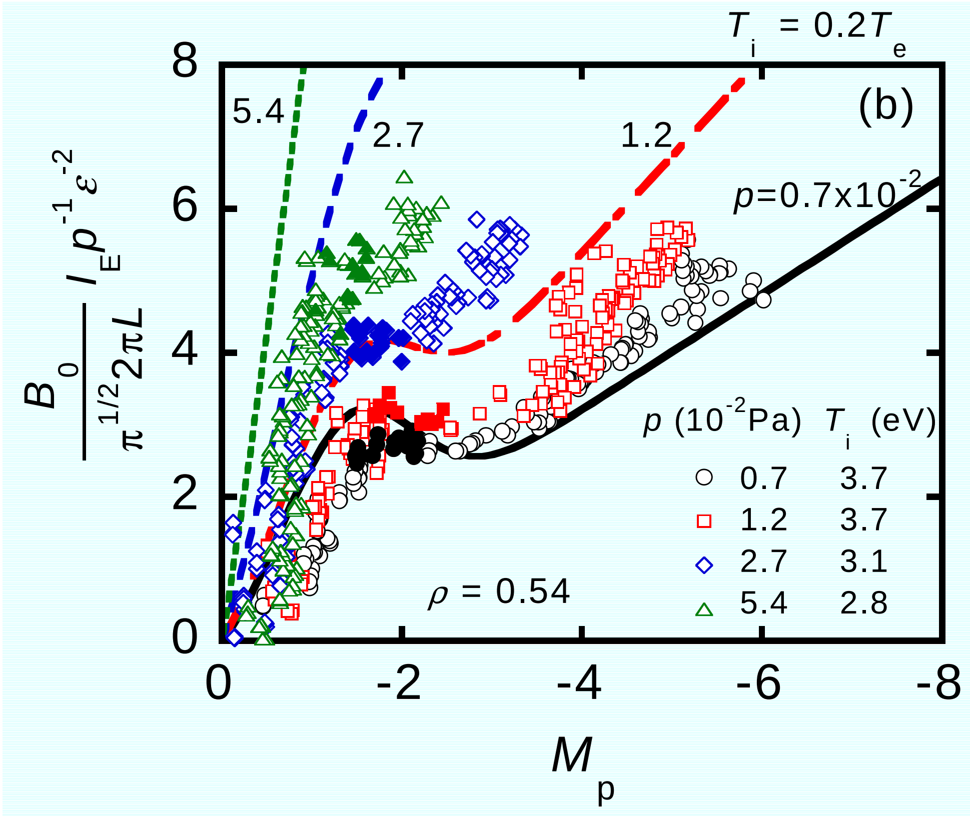

Summary

- The improved confinement mode can be triggered with both *constant voltage* and *current sweep* biasing in the Tohoku University Heliac.
- $\boldsymbol{J} \times \boldsymbol{B}$ driving force for the poloidal rotation can be controlled by the current sweep biasing.
  - Negative resistance feature was observed between the electrode current and voltage.
- The ion viscous damping force was estimated from the driving force for the poloidal rotation.
  - The measured damping force had a local maximum at the poloidal Mach number $M_p \sim 1.5$ without regard to collisionality and agreed well with the neoclassical predictions of Rozhansky model.
  - The plasma showed the negative resistance characteristics in the region where the ion viscous damping force had a local maximum.

These suggest that the L-H transition occurs near the local maximum in ion viscosity which originates from a toroidal ripple.

Dependence of the measured ion viscous damping force on the poloidal Mach number

Estimation of ion viscous damping force

→ **Subtraction of the friction from the measured driving force**

- The solid line: the ion viscous damping force of the Rozhansky[1)] model without the friction term
- The broken line: the ion viscous damping force of the Shaing[2)] model which includes a gradient of ion temperature and that of pressure and helical ripples
- These viscosities had a local maximum in the region $1 < -M_p < 3$.
- The measured viscous damping forces had a local maximum at $-M_p \sim 1.5$ and agreed well with the neoclassical predictions.
- The plasma showed negative resistance characteristics (closed symbols) in the region where the ion viscous damping force had a local maximum in $1 < -M_p < 3$.

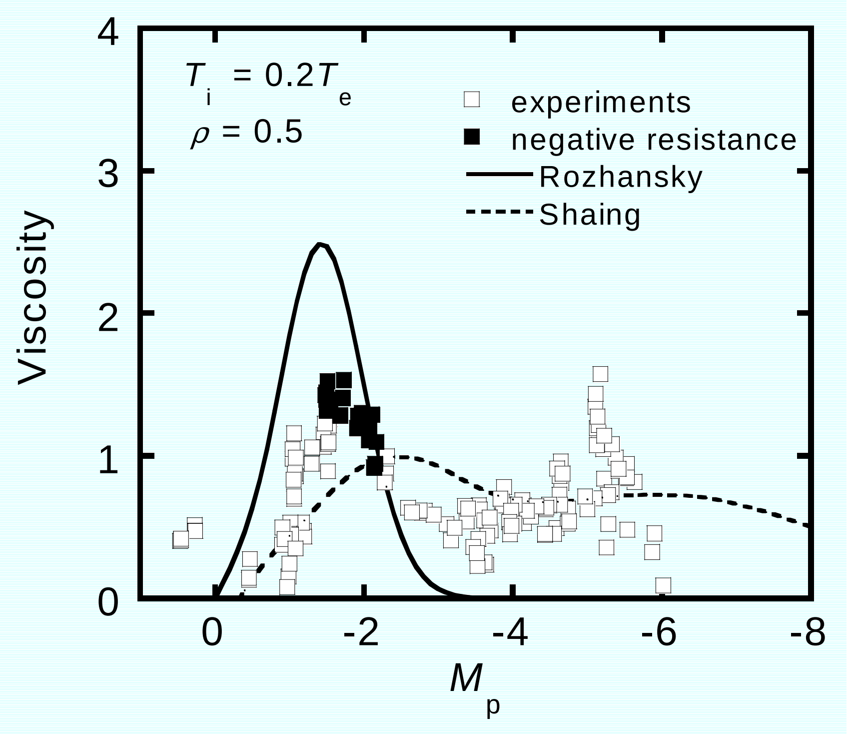

This suggested that the L-H transition occurred near the local maximum in ion viscosity which originates from a toroidal ripple and the local maxima which originate from helical ripples may not affect the L-H transition.

[1] V. Rozhansky and M. Tendler, Phys. Fluids B **4**, 1877 (1992).

[2] K. C. Shaing, Phys Fluids B **5**, 3841 (1993).

Effect of the Fourier components on the ion viscosity (1)

Magnetic configurations in Heliac can be changed widely by selection of coil current ratio.

- **Magnetic Fourier components**

r_{ax} (cm)	a (cm)	Well depth (%)	ε_{mn} $(r / R_0 = 0.05)$ (0,1)	(1,0)	(1,1)
7.3	6.3	-0.99	-0.09	-0.051	-0.060
7.5	6.6	-0.11	-0.11	-0.049	-0.056
7.9	6.8	2.3	-0.13	-0.040	-0.051
8.4	6.2	4.1	-0.16	-0.039	-0.050

These Configurations have similar profile for rotational transform.

- **Dependence of viscosity peak on the magnetic axis position**

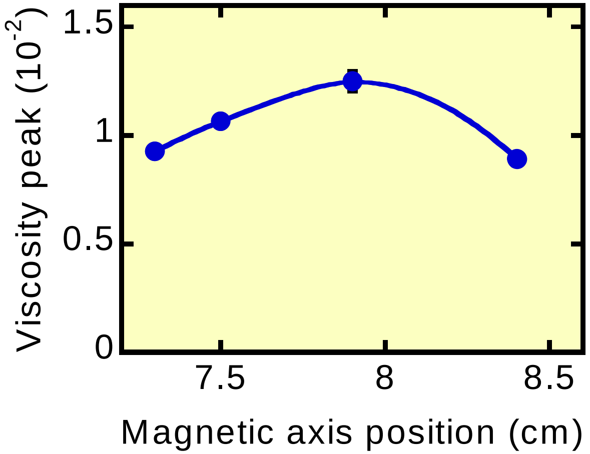

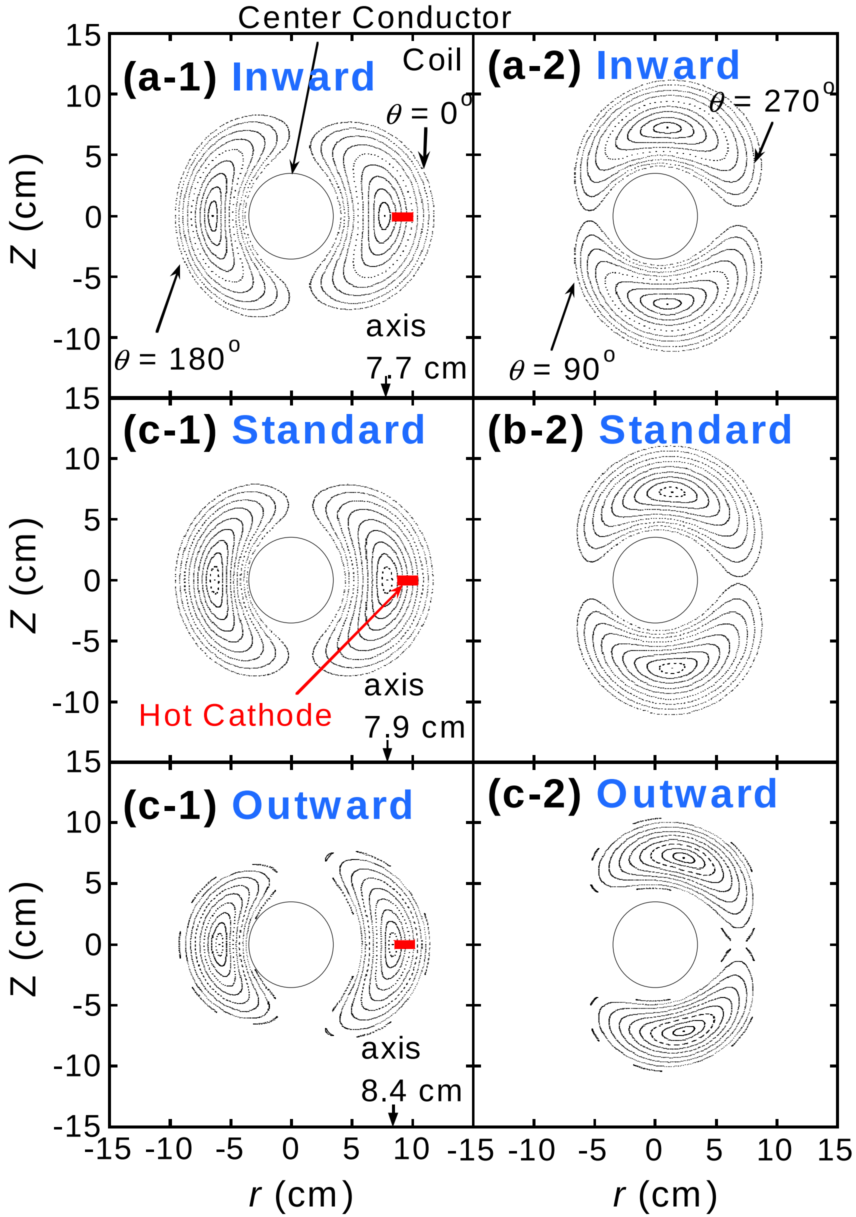

Effect of the Fourier components on the ion viscosity (2)

Estimation of poloidal ion viscosity

➡ Subtraction of the friction term from the poloidal driving force

- The theoretical ion viscosities and the measured ion viscosities had local maxima on all configurations.
- Negative resistance characteristics (closed symbols) around the ion viscosity peaks.
- The estimated peak values of viscosity agreed well with theoretical predictions.